IOP Conf. Series: Materials Science and Engineering **418** (2018) 012095 doi:10.1088/1757-899X/418/1/012095

Tool Texturing for Deep Drawing Applications

J Hazrati[1], P Stein[2], P Kramer[2], A H van den Boogaard[1]

[1] Nonlinear Solid Mechanics, Faculty of Engineering Technology, University of Twente, Enschede, The Netherlands
[2] Institut für Produktionstechnik und Umformmaschinen, Technische Universität Darmstadt, Darmstadt, Germany

j.hazratimarangalou@utwente.nl

Abstract. The application of surface texturing on sheet metal is a widely used approach to improve lubrication and control friction in deep drawing applications. However, it has been shown that current texturing processes are not robust to produce uniform textures on the sheet due to rapid and severe wear on texture-rolls. Furthermore, in multi-stage forming processes, deterioration of the sheet texture even at the first stage of forming makes texturing of the sheet metal surface ineffective. Tool surface texturing is a new method to control friction and tool wear in metal forming industry. In the current study, a multi-scale friction model is adopted to investigate the effect of tool texturing on the evolution of friction during sheet metal forming operations. The multi-scale friction model accounts for surface topography changes due to deformation of asperities and ploughing of tool asperities on the sheet metal surface, mixed lubrication regime and furthermore the tool micro-texture effects on lubricant distribution at tool-sheet metal interface. The model is validated with respect to strip-draw experiments using different tool textures. The model is later applied to the simulation of a U-bend forming process. The results show that using textured tools, it is possible to reduce friction and punch force in sheet metal forming processes. The model can be used to tailor and optimize textures on stamping tools for complex parts.

1. Introduction

In sheet metal forming processes, friction between the sheet and tools is a determining factor in the efficiency and quality of the process. It affects the formability of sheet material, tool life and the surface finish of the product. Surface texturing is an attractive approach to enhance frictional behavior and load support of contacting surfaces [1]. This method is successfully used in low load conditions such as bearings [2, 3] to reduce hydrodynamic friction where the contacting surfaces have low convergence ratio. In this method, shallow micro-pockets are incorporated deterministically or stochastically on one of the bearing surfaces using different methods such as laser beam machining, hammer peening, abrasive jet machining, electro-discharge machining, etc. These micro-pockets act as fluid reservoirs to retain a thin film of lubrication between contacting surfaces.

Skin pass rolling of the sheet metal is a widely used technique for mass production of textured sheets with stochastic pattern using electro discharged textured (EDT) rolls [4-6]. It has been shown that this method improves lubrication and reduce friction in deep drawing applications. However, the change of the texture roll surface and the loss of roughness due to wear is a major problem that effects the roughness transfer and consequently the texture configuration on the sheet metal [7]. The variation in

the sheet metal surface texture hampers the control of the friction in sheet metal forming processes. On the other hand, sheet metal products are usually formed by multi-stage forming processes. At each forming stage, sheet metal surface texture in contact with the tool is deformed. Thus, the sheet surface texture is deteriorated. This makes the texturing of the sheet metal surface ineffective for multi-stage forming processes [8].

Tool surface texturing is a new method to control friction, tool wear and improving efficiency in stamping industry [8-10]. In this method, micro-pockets are incorporated on the tool surface. It has been shown that texturing the tool surface can reduce tool wear and friction. Texturing the tool surface eliminates the problem of deterioration of sheet metal surface texture in multi-stage forming operation. Furthermore, texturing the tool surface enables to tailor the micro-pockets geometry and their distribution on the tool surface for that specific forming operation based on the local contact conditions such as contact pressure, drawing velocity and contact temperature. It was found further that the tribological behavior of these textured surfaces considerably depends on the size and distribution of these micro-pockets, whilst their shape does not significantly affect the friction coefficient regardless of rounded or angular profiles [11].

The goal of this paper is to investigate the effect of tool surface texture on its frictional behavior during forming of a sheet metal product. For this purpose, an existing micro-mechanics based friction model was adjusted to account for the hydrodynamic effects of micro-pockets on the tool surface. The model is verified relative to strip-draw tests using tools with different texture configurations. Afterwards, the validated model is used to investigate the effect of tool texturing during a U-bend sheet metal forming process.

2. Multi-scale friction model

The micro-mechanics based friction model developed by Hol, *et al.* [12, 13] is adapted to account for hydrodynamic effects of the micro-pockets on the tool surface. The model describes mixed-lubrication regime during forming processes. In mixed-lubrication regime, the friction mechanism is explained by the deformation of the asperities due to normal and sliding loads (boundary lubrication friction model), hydrodynamic effects between sheet surface asperities and tool surface and the hydrodynamic effects generated by micro-pockets on the tool surface that act as lubricant reservoir and generate lift effects.

2.1. Boundary lubrication friction model

Boundary lubrication friction model describes the evolution of frictional real area of contact due to deformation of asperities in tool-sheet metal contact. Thereby the friction is caused by adhesion and ploughing between tool surface and the sheet contact area. The sheet metal surface asperities in the contact area are flattened due to normal load, sliding of the tool over the sheet surface and straining of the underlying bulk material. At the first stage of contact, surface asperities of the rough work piece are flattened by smooth flat tool surface. The asperities are modelled as bars reconstructed from confocal measurements of the work piece representative area. Real area of contact is determined based on energy (1) and volume conservation (2) laws as described in [12].

$$p_{asp} = \frac{B}{A_{nom}}\left(\frac{\xi}{\omega} + \eta\frac{\beta}{\omega}\right) + \frac{S_{sh}}{A_{nom}}\frac{\psi}{\omega} \tag{1}$$

$$U_L\left(1 - \alpha_{asp,L}\right) = \int_{d_L - U_L}^{\infty} (z - d_L)\phi_w(z)dz \tag{2}$$

p_{asp} is the nominal contact pressure; B = 2.8, hardness parameter; $S_{sh} = 1/\sqrt{3}$, shear factor (following the Von Mises criterion) and A_{nom} the nominal contact area. ω is an external energy factor while ξ , β and ψ are internal energy factors. Complete description of the contact model can be found here [14].

As the tool slides on the work piece surface, the real area of contact increases significantly. During the flattening phase, tool asperities are penetrating on the sheet surface and as the sliding occurs, therefore only the frontal side of the asperities remain in contact with the work piece. This implies that

real area of contact, as a result, must increase by a factor of approximately 2 in order to meet the load equilibrium condition. This mechanism is known as junction growth [15].

In order to determine the friction coefficient, all the contact patches are processed and therefore, normal force and effective attack angle is determined for each contact patch. The normal force is later corrected to account for the lifting effect of micro-pockets on the tool surface, this is explained in the next section. Using Challen and Oxley's [16] slip-line theory, the friction force is determined for each single contact patch and summed up over all contact patches to find the total friction force and the shear stress (3).

$$\tau_{asp} = \frac{\sum_{n=1}^{N} \mu^n F_N}{\sum_{n=1}^{N} A^n} \tag{3}$$

N is the number of contact patches, μ^n is the friction coefficient of a single contact patch and F_N is the normal force of each contact patch.

2.2. Mixed lubrication friction model

In this study, the mixed lubrication model developed by Hol *et. al*. [13] is used to describe the hydrodynamic effects of the lubricant. The averaged Reynolds equation is solved to determine lubricant pressure and viscous shear stresses:

$$\nabla \cdot \left(\frac{h^3}{12\tau} \boldsymbol{\Phi_p} \cdot \nabla p_{lub} \right) = \nabla \cdot \left(\frac{h(v_1 + v_2)}{2} + \frac{S_q}{2} (\mathbf{v_1} - \mathbf{v_2}) \cdot \boldsymbol{\Phi_s} \right) + \frac{\partial h}{\partial t} \tag{4}$$

Where p_{lub} is the hydrodynamic pressure in the fluid; η the dynamic viscosity; h the fluid film thickness and S_q the surface roughness of the undeformed surfaces. $\mathbf{v_1}$ and $\mathbf{v_2}$ are the velocities at the tool and work piece surfaces.

To solve the hydrodynamic pressure distribution from the averaged Reynolds equation, lubricant flow is coupled to the surface roughness evolution via calculating the lubricant film area and thickness based on the flattening and rise of asperities and the lubricant amount at the contact. Flattening and rise of asperities are calculated from boundary lubrication friction model. Finally, viscous shear stresses for a Newtonian lubricant is calculated using:

$$\tau = \eta \frac{\partial \mathbf{v}}{\partial z} = \eta \frac{\mathbf{v_2} - \mathbf{v_1}}{h} + \frac{2z - h}{2} \nabla p_{lub} \tag{5}$$

The total shear stress (τ_{tot}) is the sum of shear stresses between contacting asperities (3) and lubricant shear stress (5). Therefore, friction coefficient is calculated as:

$$\mu = \frac{\tau_{tot}}{p_{nom}} \tag{6}$$

p_{nom} is the nominal contact pressure.

The lift effect of the micro-pockets on the tool surface is modeled by summing the normal lifting forces that are generated at the outlet of each micro-pocket. The confocal image of the micro-pockets on the tool surface generated by machine hammer peening method and a schematic of a trapezoidal micro-pocket on the tool surface are shown in figure 1. In this study, three different tool textures are generated by varying the distance between indentations [9]. Specifications of the tool textures are given in table 1.

Normally, there is a significant external pressure at the inlet of the micro-pocket however as the lubricant enters the pocket, its pressure drops significantly. This results in sucking the lubricant into the contact. As the increased flow reaches the rear end of the pocket, a larger peak pressure is generated. The increase in the pressure at the rear end (outlet) of the pocket produces a separating load at the contacting surfaces. The lifting effect is analyzed in full by equating the flows through the three parts of the micro-pocket: inlet, pocket surface and outlet. The load carried by a single pocket is derived from equation (7) that is adopted from [17]. In the current model, solely the lifting effects of the tool texture are taken into account and the hydrodynamic effects of sheet metal surface texture are not considered. Therefore, it is assumed that no cavitation occurs in the micro-pockets of the sheet metal surface. This

can be a fair assumption since the micro-pockets generated by EDT rolls on the sheet metal surface are well interconnected [7] that reduce the lifting effects of these micro-pockets.

The lifting (support) load produced by the individual micro-pockets on the tool surface is summed over the contact area filled with lubricant and multiplied by the fraction of the tool that is covered with the micro-pockets.

$$F_{N,pocket} = 6v\eta \frac{(h_p - h_0)ab}{(2ah_p^3 + bh_0^3)} \; A_{lub} \; \alpha_{tex} \tag{7}$$

v is the uniform relative velocity of the surfaces; A_{lub}, lubricant film area; α_{tex}, percentage of area covered by micro-pockets and η is the dynamic viscosity. a, b, h_0 and h_p are micro-pocket dimensions shown in figure 1.

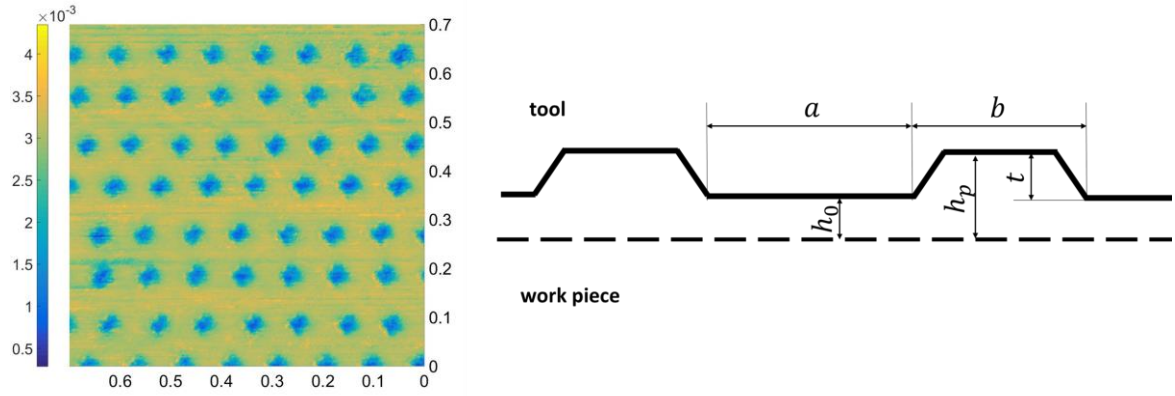

Figure 1. Confocal image of the textured tool surface with texture coverage area of 25% (left), and micro-pocket parameters (right).

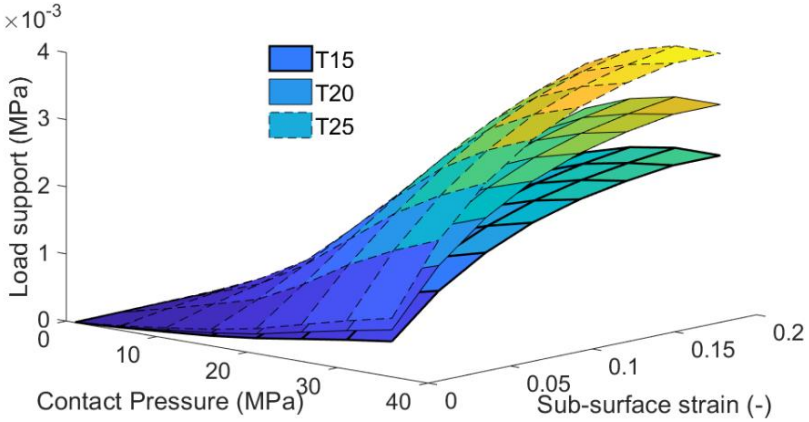

Figure 2. Micro-pocket pressure profile as a function of nominal pressure and sub-surface strain.

As mentioned previously, lubricant film thickness is calculated based on deformation of asperities and amount of lubricant at the contact. Therefore, h_0 is a function of nominal contact pressure and the sub-surface strain in the sheet metal. h_0 decreases as the contact pressure and sub-surface strain increase. Figure 2 shows the effect of nominal contact pressure and sub-surface strain on the load carrying capacity of the micro-pockets at the tool surfaces with different texture coverage area. The curve shows that for higher contact pressures and strains in the work piece, the micro-pockets are more effective by carrying higher loads.

If the lubricant starvation happens at the contact surface, the lifting effect of micro-pockets is not taken into account. However, taking the lubricant amount of 2 g/m^2, no starvation of lubricant at the contact was observed for the surfaces investigated in this study.

3. Strip draw tests

3.1. Experiments

In order to investigate the effect of tool texturing on frictional behaviour of tool-sheet metal tribological system, strip-draw tests are used. Textured surfaces of the tools for strip-draw tests were produced using hammer peening method as described earlier (table 1). Trapezoidal micro-tips were used to produce equidistant micro-indentations with a constant hammering frequency of 120 Hz on the tool surface with milling finish (tool steel: X153CrMoV12). This results in deterministic micro-textures on the tool surface while initial surface asperities are significantly flattened. By varying the distance between micro-indentations, 3 tool surface textures with different surface coverage areas of 15, 20 and 25% were produced. The resulting tool surfaces were investigated with the confocal white light microscope µ-Surf from nanofocus. All measurements are horizontally adjusted to avoid influences of possible profile inclinations [9]. The measured surface is corrected for tilt or curvature and a noise filter is used to remove the spikes [13]. Table 1 shows the average dimensions of the micro-indentation for trapezoidal micro-tip.

To compare the frictional behaviour of textured tool surfaces with an un-textured tool surface, one pair of tools is hardened to 65 HRC and polished to Ra = 0.03 µm that is smoother than tool roughness used in common stamping dies. The latter is used as the reference.

Table 1. Roughness of the tools and pocket dimensions for three different tool textures.

Tools	Ra (μm)	Texture area	$\boldsymbol{a}$ (μm)	$\boldsymbol{b}$ (μm)	$\boldsymbol{t}$ (μm)
T15	0.17	15%	130.5	42.9	6.1
T20	0.15	20%	109.8	42.9	6.1
T25	0.17	25%	92.3	42.9	6.1
Polished	0.03	-	-	-	-

Figure 3 shows the results of strip draw tests on galvanized and EDT-structured strips of dual phase steel (DP800) using textured tool blocks. A mineral oil-based pre-lubricant (PL61, Zeller-Gmelin, Eislingen/Fils, Germany) with viscosity of υ = 58 mm^2/s at 40 ºC, density d = 0.9 g/cm^3 at 15 ºC is used. The strips are drawn with a constant velocity of 50 mm/s over a 100 mm length. The tests were erformed at two nominal contact pressures of 4 and 8 MPa.

3.2. FE Simulations

The strip draw tests were simulated using an in-house finite elements method software (DiekA, University of Twente). The friction model described in the previous sections was used taking the strip material properties, surface height data of tool and strips and lubricant properties into account. Elasto-plastic material behaviour of the zinc coating (8) is derived from the load-displacement curves of Nano-indentation test by Song *et al.* [18].

$$\sigma_y = \sigma_0 \left(1 + \frac{E\varepsilon_p}{\sigma_0}\right)^n \tag{8}$$

Where ε_p is plastic strain, E = 70 GPa is Young's modulus, σ_0 = 75 MPa is the initial yield strength and n = 0.14.

Figures 3 shows the coefficient of friction obtained from finite element (FE) simulation of strip draw tests and its evolution versus the drawing distance. The polished tool surface results in the lowest friction coefficient while the tool with the least textured area (T15, 15%) leads to the highest friction for both

contact pressures. Figure 3 shows that FE results are able to replicate the experiments with fair accuracy, however, the FE results of T20 tool is less favorable to experiments and results in an error of 17%. This might be due to the fact that lifting effects of the micro-pockets at lower pressures is underestimated in the current model. Furthermore, the experimental results depicts that the friction coefficient slightly increases for the T25 tool with larger texture coverage area, this is also reproduced by FE results. This increase can be explained by its slightly higher roughness relative to T20 tool (table 1). Figure 4 depicts the distribution of friction coefficient and lubricant pressure during strip-draw tests using polished tool surface and texture tool T20 for contact pressure of 8 MPa. Lubricant pressure for the textured tool is slightly higher than the polished one. The latter implies that ploughing friction forces are much higher for the textured tool case.

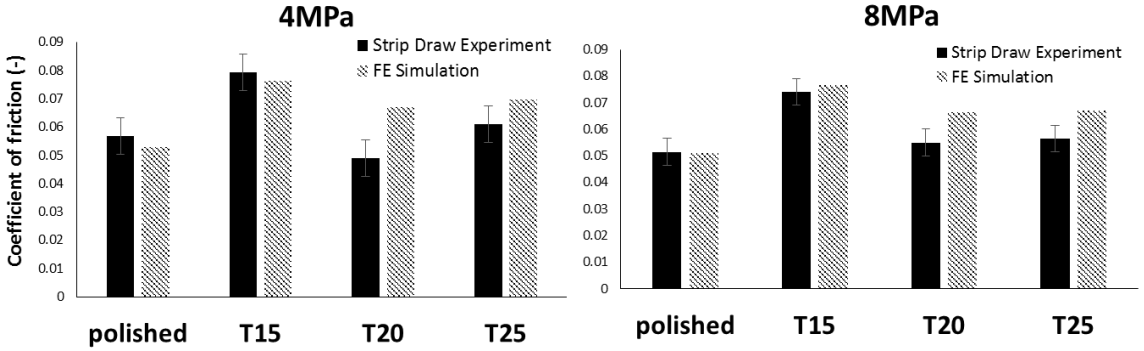

Figure 3. Strip draw experiments and FE simulation results at contact pressures of 4 and 8 MPa.

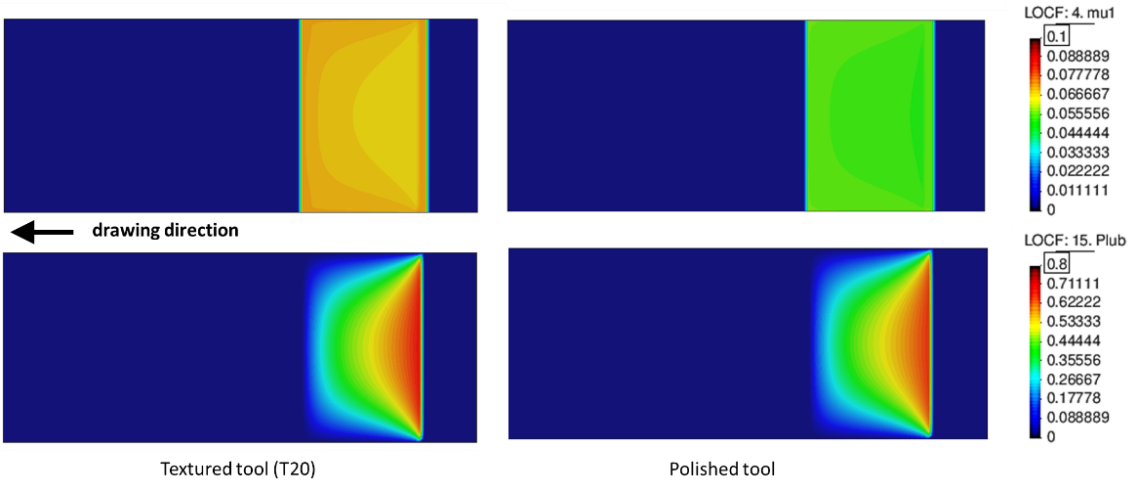

Figure 4. Friction coefficient (top row) and lubricant pressure [MPa] (bottom row) distribution during strip draw test using textured tool, T20 (left column) and polished tool (right column) for contact pressure of 8 MPa.

4. U-bend forming

The developed model is used in forming simulation of a U-bend forming process. The FE model is first validated relative to an experiment using an un-textured tool setup Ra = 0.04 µm [13]. The specifications of the experiments and FE simulations can be found in table 2. The amount of lubricant is fixed at 2 g/m^2 to ensure the mixed lubrication and avoid the lubricant starvation on the contact interface.

Uncoated sheet metal DC06 (Ra = 1.4 µm) is used in these experiments, this means that the friction model is adapted to account for the material behavior of steel in friction calculations. Vegter yield criterion and Bergström-van Liempt hardening rule is used to describe the material behavior of DC06 in the friction model as well as the FE model, the constants of the model can be found in [12]. Due to

symmetry, a quarter of the U-bend is modeled in FE simulations. Force-displacement curves are used to compare the FE results with the experiments.

The results show that FE results compare fairly well with the experiment (figure 5). The validated model is used to investigate the effect of tool texture on behavior of the system. The three tool textures with different surface area coverage as used in the strip-draw tests are used in FE simulation of U-bend process.

The results show that using textured tools the friction coefficient significantly drops and leads to lower forming forces (figure 5). As shown above, the load carrying capacity of the micro-pockets on the tool increases with increasing contact pressure and strain in the work piece. Therefore, it is expected that tool texture would play a more significant role in forming operation than strip drawing test where the nominal contact pressure is 4-8 MPa. However, the results show that different tool textures with different texture coverage area do not lead to a notable difference in force-displacement curves. Figure 6 shows the friction coefficient distribution on the U-bend section at the punch-blank holder side where the textured tool show significantly low friction coefficient with respect to polished tool.

Table 2. Parameters of U-bend forming process.

Parameter	**Specification**
Blank material	DC06 EN10130:2006
Tool material	DIN 1.2379
Lubricant	Quaker FERROCOAT® N6130 ($\eta_{40^\circ} = 23$ mPa.sec)
Lubrication amount	2.0 g/m^2
Blank geometry	300 x 25 x 0.8 mm
Blank holder force	25 kN
Punch velocity	50.0 mm/s
Drawing depth	75 mm

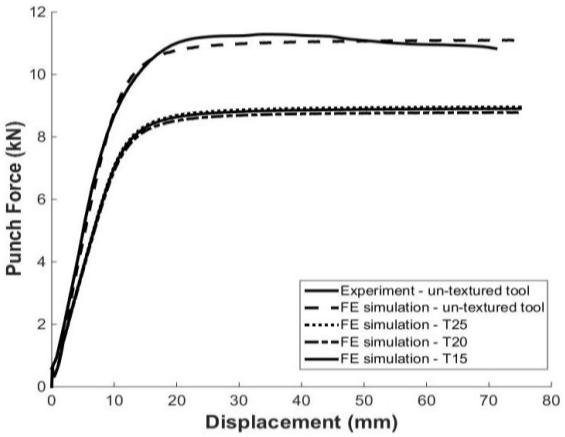

Figure 5. Force-displacement curves of U-bend forming operation.

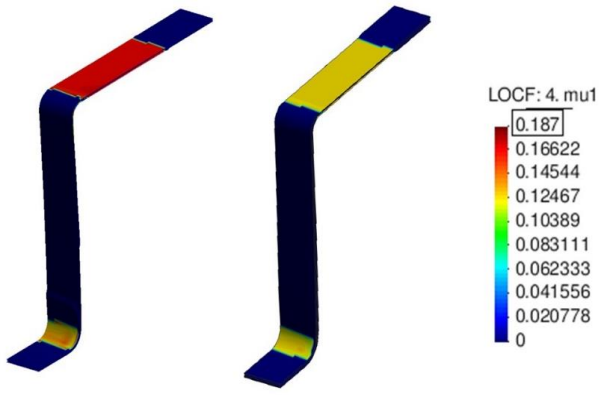

Figure 6. Distribution of friction coefficient at the last increment of U-bend forming using the un-textured (right, Ra = 0.04 μm) and textured tool T20 (left, Ra = 0.15 μm).

5. Conclusion

In the current study, a multi-scale friction model [14] is used to investigate the effect of tool surface texturing on the evolution of friction during strip draw test and U-bend forming application. The experimental and numerical results show that texturing of the tool surface is an effective way to reduce friction in the tool-work piece contact and thereby reducing the forming force and tool wear. In the current model, load carrying capacity of micro-pockets on the tool surface was taken into account using

an analytical solution for a 2D profile, however this needs to be further improved to account for 3D geometry of the micro-pockets. Moreover, the micro-pockets so far are expected to mainly function in hydrodynamic lubrication conditions and therefore the effect of these micro-pockets in boundary lubrication condition where lubricant starvation may happen in the micro-pockets is still unexplored. Finally, the current framework can be used to tailor and optimize texture configuration in the stamping tools.

References

[1] Kovalchenko A, Ajayi O, Erdemir A, Fenske G and Etsion I 2005 The effect of laser surface texturing on transitions in lubrication regimes during unidirectional sliding contact *Tribology International* **38** 219-25
[2] Rahmani R and Rahnejat H 2018 Enhanced performance of optimised partially textured load bearing surfaces *Tribology International* **117** 272-82
[3] Gropper D, Harvey T J and Wang L 2018 A numerical model for design and optimization of surface textures for tilting pad thrust bearings *Tribology International* **119** 190-207
[4] Simão J, Aspinwall D K, Wise M L H and El-Menshawy M F 1994 Mill roll texturing using EDT *Journal of Materials Processing Technology* **45** 207-14
[5] Elkoca O 2008 A study on the characteristics of electrical discharge textured skin pass mill work roll *Surface and Coatings Technology* **202** 2765-74
[6] Kijima H and Bay N 2008 Skin-pass rolling I—Studies on roughness transfer and elongation under pure normal loading *International Journal of Machine Tools and Manufacture* **48** 1313-7
[7] Wentink D J, Matthews D, Appelman N M and Toose E M 2015 A generic model for surface texture development, wear and roughness transfer in skin pass rolling *Wear* **328-329** 167-76
[8] Sulaiman M, Christiansen P and Bay N 2017 The Influence of Tool Texture on Friction and Lubrication in Strip Reduction Testing *Lubricants* **5** 3
[9] Steitz M, Stein P and Groche P 2015 Influence of Hammer-Peened Surface Textures on Friction Behavior *Tribology Letters* **58** 24
[10] Groche P, Engels M, Steitz M, Müller C, Scheil J and Heilmaier M 2012 Potential of mechanical surface treatment for mould and die production *International Journal of Materials Research* **103** 783-9
[11] Wakuda M, Yamauchi Y, Kanzaki S and Yasuda Y 2003 Effect of surface texturing on friction reduction between ceramic and steel materials under lubricated sliding contact *Wear* **254** 356-63
[12] Hol J, Meinders V T, de Rooij M B and van den Boogaard A H 2015 Multi-scale friction modeling for sheet metal forming: The boundary lubrication regime *Tribology International* **81** 112-28
[13] Hol J, Meinders V T, Geijselaers H J M and van den Boogaard A H 2015 Multi-scale friction modeling for sheet metal forming: The mixed lubrication regime *Tribology International* **85** 10-25
[14] Hol J 2013 *Multi-scale friction modeling for sheet metal forming*: University of Twente)
[15] Tabor D 1959 Junction growth in metallic friction: the role of combined stresses and surface contamination. In: *Proc. R. Soc. Lond. A*: The Royal Society) pp 378-93
[16] Challen J M and Oxley P L B 1979 An explanation of the different regimes of friction and wear using asperity deformation models *Wear* **53** 229-43
[17] Fowell M, Olver A, Gosman A, Spikes H and Pegg I 2007 Entrainment and inlet suction: two mechanisms of hydrodynamic lubrication in textured bearings *Journal of Tribology* **129** 336-47
[18] Song G M, Sloof W G, Pei Y T and De Hosson J T M 2006 Interface fracture behavior of zinc coatings on steel: Experiments and finite element calculations *Surface and Coatings Technology* **201** 4311-6